



Vascular endothelial profilin-1 Inhibition suppresses tumor progression in renal cancer

David M. Gau¹, Abigail Allen¹, Andrew Daoud¹, Jessica Kunkel¹, Anurag N. Paranjape², Flordeliza S. Villanueva^{2,3}, Partha Roy^{1,3}

¹: Bioengineering, University of Pittsburgh ²: Medicine, Division of Cardiology, University of Pittsburgh ³: UPMC Hillman Cancer Center

Abstract

Background. Clear-cell renal cell carcinoma (ccRCC) is the most common subtype of renal cancer with poor patient prognosis. A distinguishing hallmark of ccRCC is the highly vascularized tumor microenvironment caused by loss of the Von-Hippel Lindau (VHL) gene. Current anti-angiogenic therapies, while initially effective, do not display long-term therapeutic benefit with almost all patients developing drug-resistant disease. We previously discovered dramatic transcriptional upregulation of actin-binding protein profilin-1 (Pfn1) in tumor-associated vascular endothelial cells (VEC) and higher expression of Pfn1 correlated with poor patient outcome in human ccRCC. The goal of the present study was to further investigate whether vascular endothelial Pfn1 promotes tumor progression in renal cancer.

Methods. To induce wide-spread loss of Pfn1 function selectively in VEC, we engineered mice with tamoxifen-inducible excision of the Pfn1 gene by Cre driven by CDH5-promoter. For restricting loss of vascular endothelial Pfn1 to kidney only, we performed sub-capsular injection of adenovirus encoding Cre (Ad-cre) driven by CDH5 promoter, with Ad-GFP administration serving as control. Orthotopic tumor was established by sub-capsular injection of RCC cells in the kidney of syngeneic immunocompetent mice. Tumor angiogenesis and apoptosis of cancer cells were assessed by CD31- and TUNEL-staining of tumor histosections. Novel inhibitor of the Pfn1-actin interaction (Pfn1i) was discovered by computationally guided biochemical screen of small molecules followed by structure-activity relationship assays to identify improved analogs.

Results. We found that triggering endothelial Pfn1 deletion, either globally or restricted to kidney only, dramatically inhibits tumor formation and metastatic dissemination from syngeneic transplants of RCC cells. Loss of endothelial Pfn1 led to a major suppression of tumor angiogenesis ensuing massive tumor cell death. In a delayed induction setting, loss of endothelial Pfn1 also retarded progression of pre-established tumors. Consistent with these genetic proof-of-concept findings, we further demonstrated capability of Pfn1i to inhibit aggressiveness of RCC cells *in vitro*, reduce tumor angiogenesis and tumor growth *in vivo*. Furthermore, toward the goal of targeted delivery of Pfn1i in tumor microenvironment, we have successfully encapsulated Pfn1i into lipid microbubbles, and demonstrated proof-of-concept for prominent anti-angiogenic action by Pfn1i in cell culture setting released by ultrasound-mediated disruption of microbubbles. These findings lay the groundwork for our ongoing effort focused on localized ultrasound-guided delivery of Pfn1i in tumor microenvironment as a therapeutic strategy in mouse model of RCC.

Adverse association of Pfn1 with patient outcome in human ccRCC

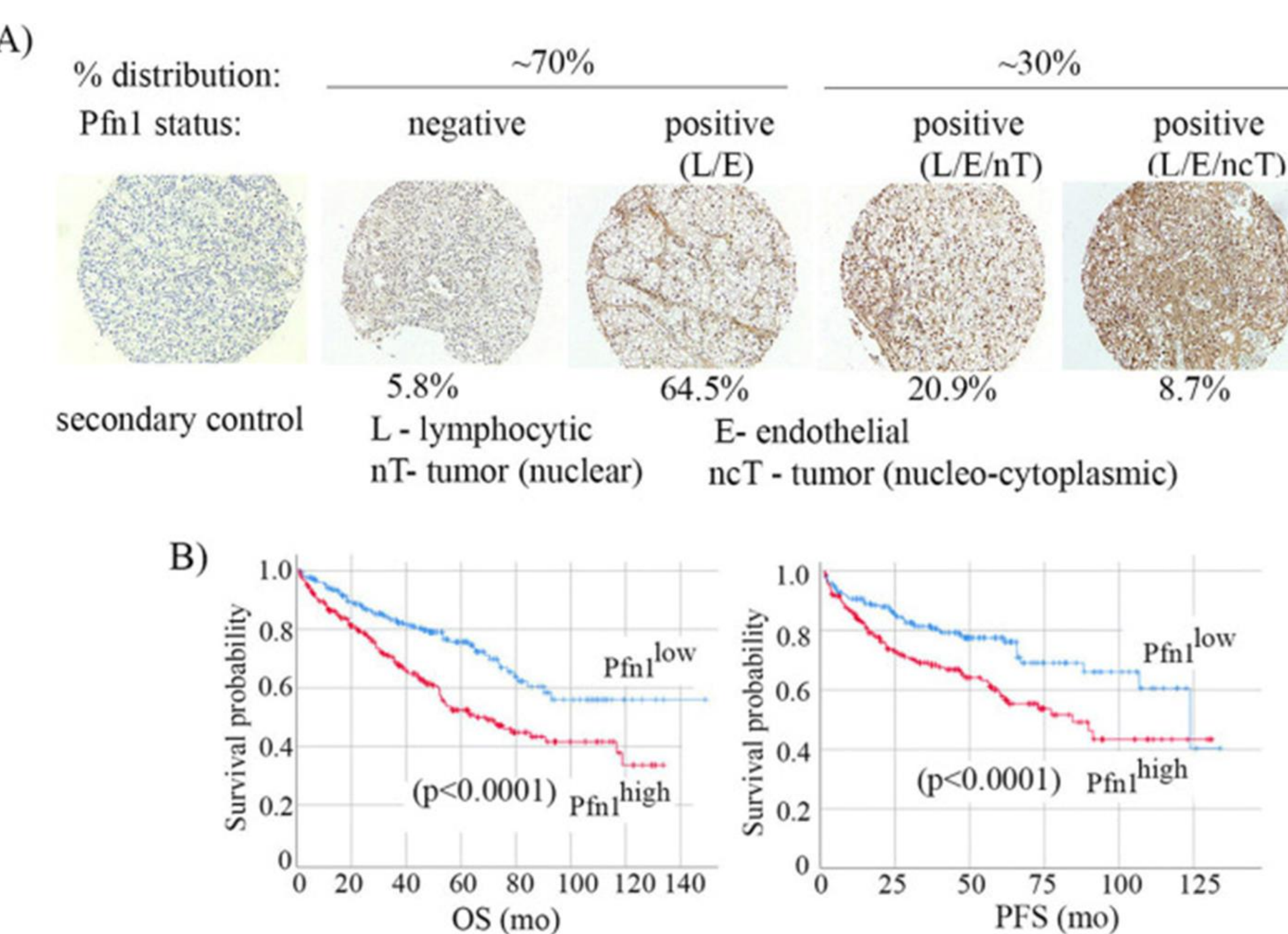


Fig 1. A) Pfn1 IHC of ccRCC TMAs showing frequency of tumors with different expression patterns of Pfn1 (n = 417 tumors) (blue, nuclei). **B)** survival (OS and PFS) of ccRCC patients (these data are based on the analyses of TCGA data representing 537 clinical cases). $***, p < 0.0001$. Samples with missing stage, grade, and metastasis information were excluded (numbers in parentheses in B denote number of clinical cases in each category). For survival analyses (available for all 537 patients), transcript expression was dichotomized at the median value. Red and blue lines in Kaplan-Meier survival plots indicate higher and lower than median expression, respectively. Data published in [1].

Loss of endothelial Pfn1 leads to reduced tumor progression and metastatic burden

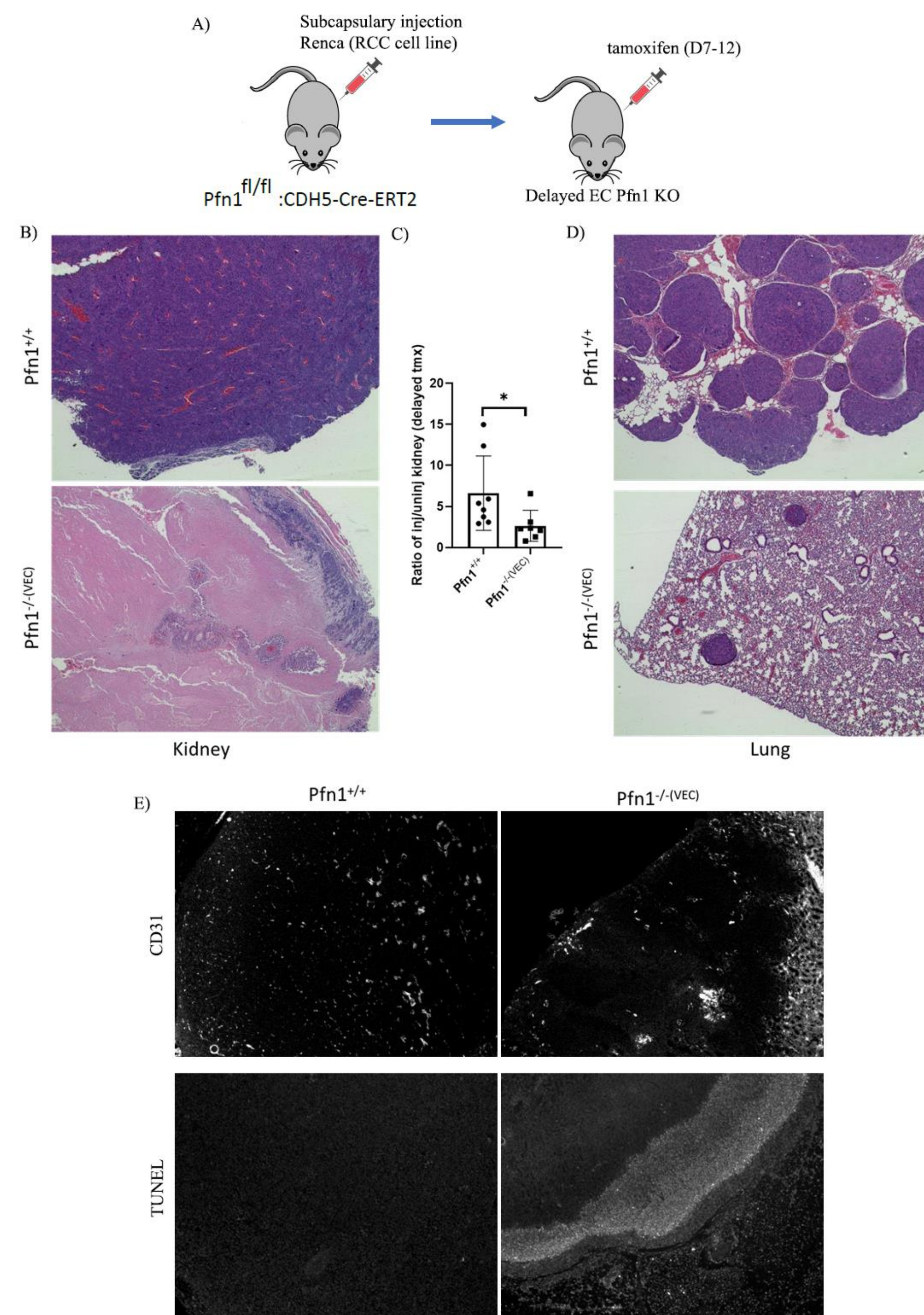


Fig 2. A) Schematic layout for delayed VEC Pfn1 deletion starting from D7-D12 of tumor injection. **B)** H&E of tumors on D28 after tumors were allowed to form in mouse kidney for 7-10 days prior to treatment with tamoxifen showing that loss of endothelial Pfn1 increases tumor necrosis and less tumor angiogenesis. **C)** Quantification of tumor injected kidney over non-injected kidney depicting that loss of endothelial Pfn1 leads to smaller tumor formation, $* p < 0.05, N = 8$. **D)** H&E of lung metastasis on D28 depicting that loss of endothelial Pfn1 leads to reduced metastatic burden. **E)** Representative immunostaining images for CD31 and TUNEL of delayed Pfn1 VEC KO in tumor regions.

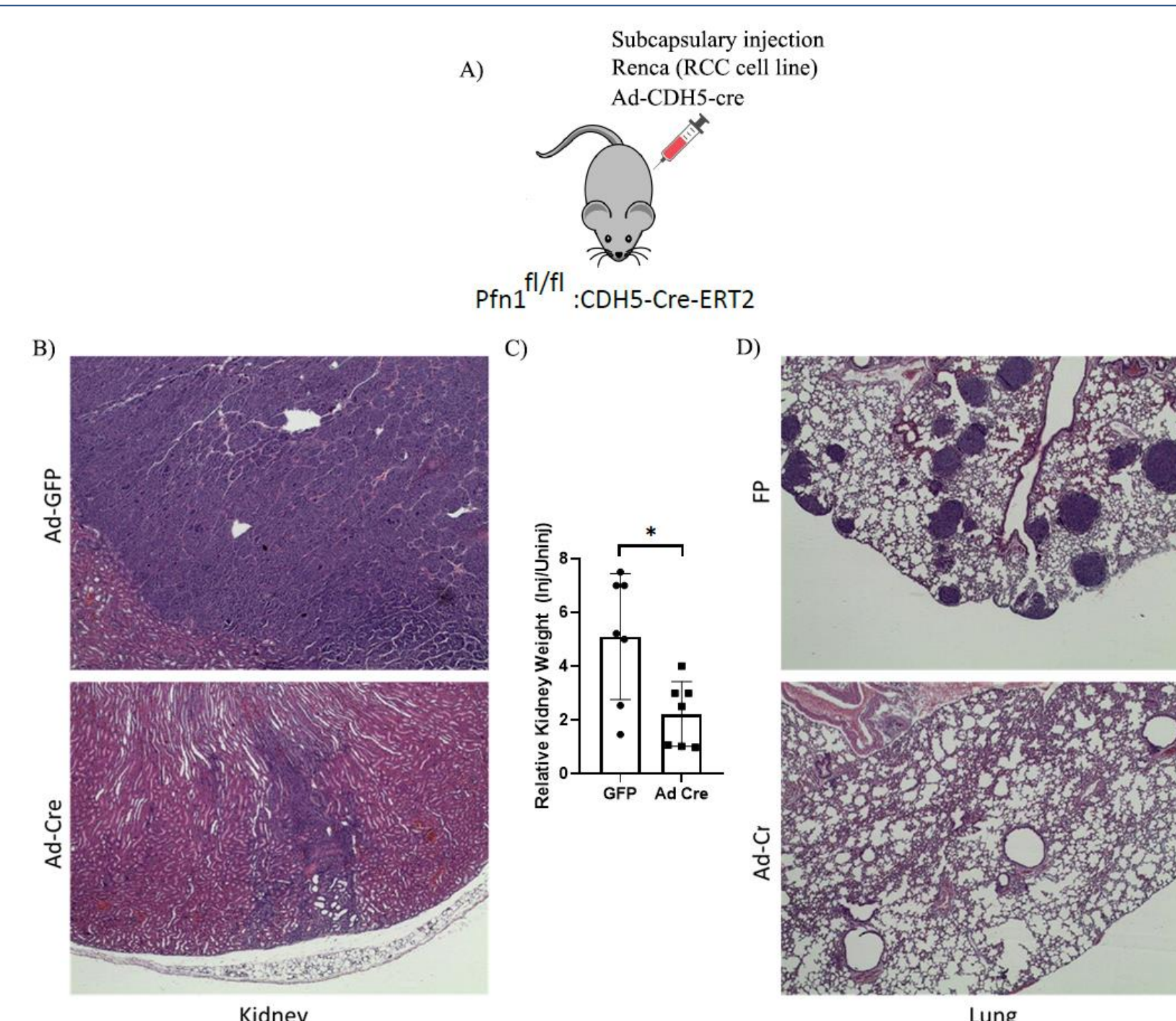


Fig 3. A) Schematic layout for local deletion of VEC Pfn1 starting from D0 of tumor injection. **B)** H&E of tumors on D14 from tumors injected into mouse kidney with Ad-GFP or Ad-Cre showing that loss of endothelial Pfn1 reduces tumor burden. **C)** Quantification of tumor injected kidney over non-injected kidney depicting that loss of endothelial Pfn1 leads to smaller tumor formation, $* p < 0.05, N = 7$. **D)** H&E of lung metastasis on D14 depicting that loss of endothelial Pfn1 leads to reduced metastatic burden.

Demonstration of Pfn1 inhibitor's (C74) ability to reduce RCC cell proliferation *in vitro* and tumor growth *in vivo*

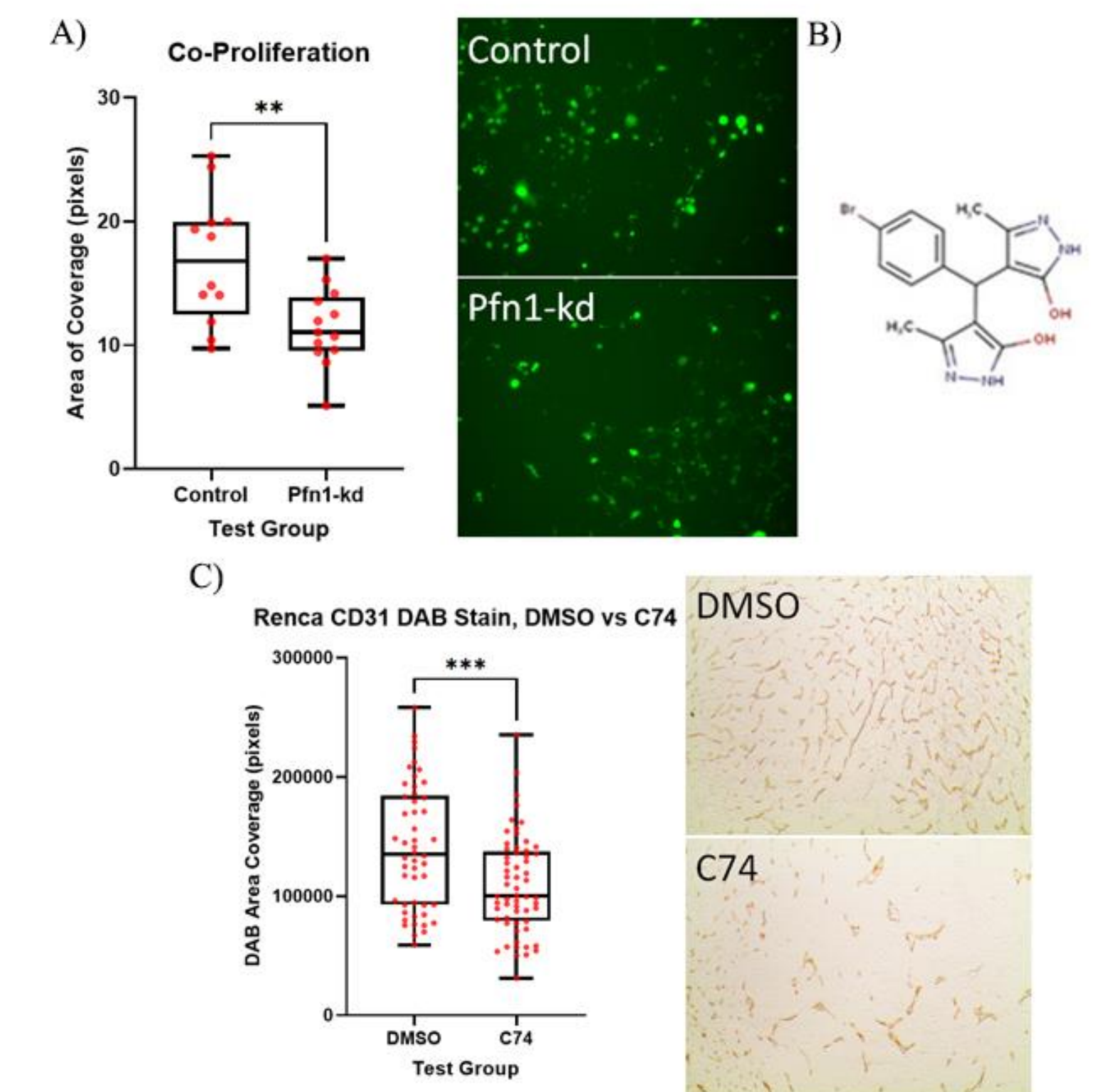


Fig 4. A) Box plots and representative images summarizing the results of co-culture of RCC cells and VEC with or without Pfn1 on RCC proliferation after 4 days. **B)** Diagram of C74, the highest scoring Pfn1:actin inhibitor by *in silico* and *in vitro* techniques. **C)** Box plots and representative CD31 stained Matrigel plug with or without C74 images summarizing the results of RCC cells injected subcutaneously into the flank of Balb/C mice. $** p < 0.01$.

Ultrasound-induced cavitation of microbubble dosed with Pfn1i reduces cord formation

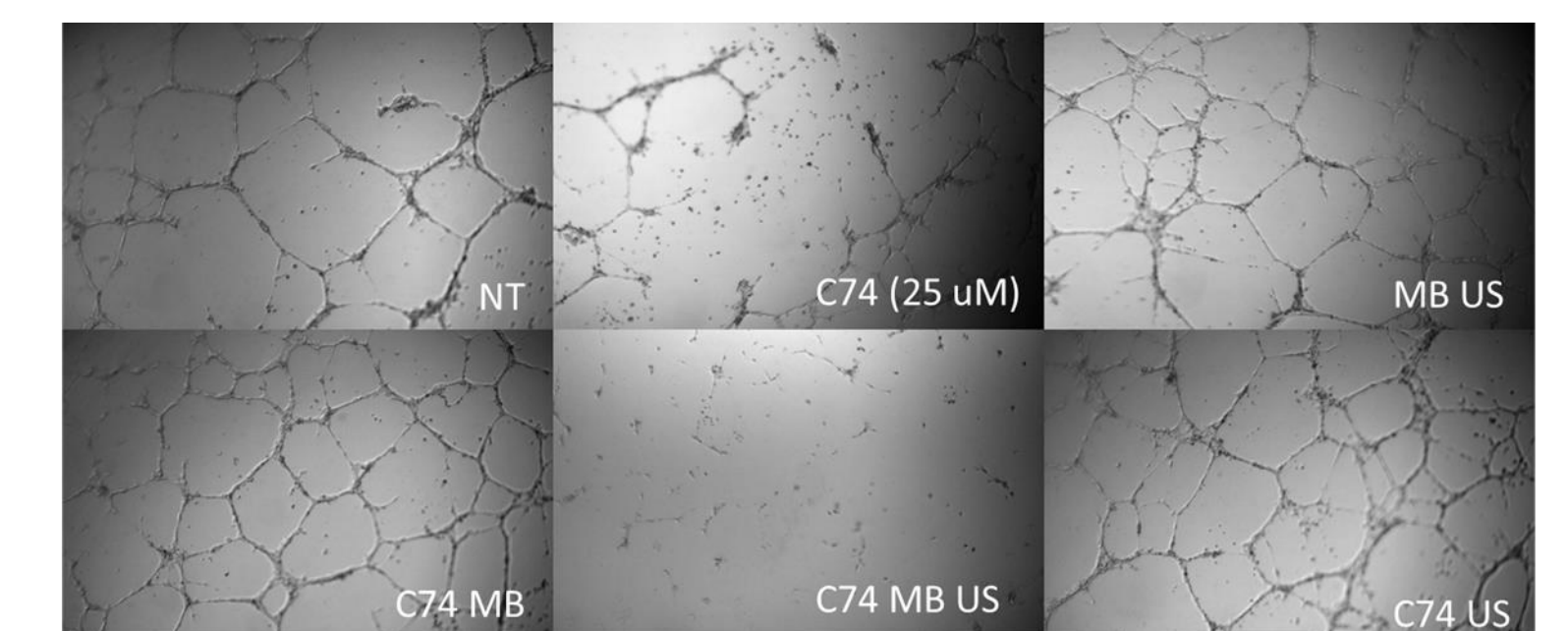


Fig 5. Representative images of cord formation from HmVEC treated with DMSO, Pfn1i (C74), empty microbubble (MB), C74 MB with no ultrasound, C74 MB with ultrasound, C74 treatment only during ultrasound. MB US control shows that ultrasound-induced cavitation of microbubble does not cause defect in cord formation. C74 MB control shows that C74 dosed microbubbles without ultrasound cavitation has no impact on cord formation. C74 US control shows that ultrasound does not promote C74 absorption into cells (C74 is only present while ultrasound occurs).

Conclusions

- Pfn1 is associated adversely with ccRCC patient outcome
- Loss of Pfn1 in VEC reduces RCC tumor burden
- Pfn1i can inhibit tumor progression and vascularization *in vivo* and *in vitro*

Acknowledgements

The authors wish to acknowledge the grant support from the National Institute of Health (R01-CA248873) to PR and NIH (T32-HL129964 and K99-CA267180) to DG.

References

1. Allen A, Gau D, et al. J Biol Chem. 2020. doi: 10.1074/jbc.RA120.013963